Analytical Modeling and Design Criteria for Traveling-Wave FET Amplifiers

Stefano D'Agostino, Guglielmo D'Inzeo, *Member, IEEE,* and Luca Tudini

Abstract—**This paper describes the theoretical modeling and design of a traveling-wave FET. The device shows the capability of wide-bandwidth performance, high gain, and could be useful in power applications. The proposed analytical model considers the full modal effects of the three-coupled transmission lines and an accurate analysis of the FET model in the traveling-wave amplifier. Starting from electrode dimensions and active zone doping, such a model allows one to calculate the scattering parameters. Thus, it is possible to analyze the device as a six port network in a circuit analysis program.**

I. Introduction

TRAVELING-wave field-effect transistor (TWF) is a solid state device designed to amplify signals over a wide bandwidth [1]. TWF makes use of an exponentially growing wave mode, which grows along the device length (W) (Fig. 1), through a distributed interaction mechanism based on the active characteristics of the transistor.

McIver firstly suggested a microwave distributed amplifier using a unipolar device [2]. In such a case, a field-effect transistor with insulated gate (MOSFET) is used as an active component. It consists of three principal components: input line, output line and a FET active structure that couples both lines. The coupling between the lines is analyzed considering only the active part. In the following, to obtain a gain growing by increasing the device length, some different solutions have been suggested [3], [4]. In these studies, mutual inductance and capacitance of the lines have not been included, and an assumption of small losses has been made.

The first TWF fabrication was carried out by Holden [5], who achieved a negative attenuation constant by adding lumped capacitances between drain and source. These capacitances have the same value of the FET junction capacitance and are periodically placed at such a distance that they can be seen by the signal as a distributed overlay capacitance. The amplifier is 3 mm long with a 1 μm wide gate. The analysis is developed according to transmission line theory and the results prove the device's reciprocal behavior.

We have previously proved that it is impossible to obtain modes with a negative attenuation constant (i.e., α)

Manuscript received August 15, 1990; revised July 13, 1991.

The authors are with the Department of Electronics, University "La Sapienza" of Rome, Via Eudossiana 18, 00184, Rome, Italy.

IEEE Log Number 9104768.

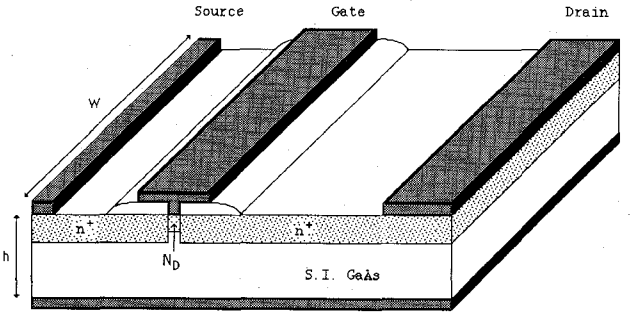

Fig. 1. Tridimensional global view of the TWF.

in a normal MESFET configuration, and it is necessary to use a T-shape cross section of the gate [1].

Recently a new realization has been proposed by Sebati *et al.* [6], the theoretical study has been developed using the transmission line methodology. The suggested TWF has a T-gate, to reduce resistive losses, and a Schottky contact at the drain-side, that allows an increase of the capacitance between drain and source to get amplification. In a 1.2 mm long device a 5 $\pm$ 2 dB gain was obtained in the band between 1 and 5.7 GHz.

In this work we analyze the TWF behavior, showing the possibility of growing waves propagation. The optimization of the structure dimensions, such as the use of a T-shape gate, allows amplification over a wide bandwidth.

II. Theoretical Analysis

Fig. 1 shows a schematic representation of the TWF. The device has three coupled electrodes, placed on a thin layer of gallium arsenide (GaAs) substrate. A semi-insulating GaAs substrate supports the electrodes. Just as in a common FET, the three electrodes are the source, the gate, and the drain.

Owing to the complexity of this structure some authors simplify the problem considering the coupling between the lines only by means of a transconductance. However, this approach doesn't given good results [7].

In this work, the structure is analyzed considering the electrodes as multicoupled microstrip transmission lines (width W_m) and the equivalent circuit of the FET active region as distributed along the device length (W). To use the transmission line theory, it is necessary to find the distributed equivalent circuit of the TWF. In the next

paragraph capacitance and inductance matrices per unit length of the lines are calculated. These matrices represent the mutual coupling between the lines, which is only due to the presence of the three electrodes. Afterwards, the contribution that the active part of the TWF gives to the equivalent circuit is considered.

After obtaining all the quantities of the equivalent circuit (Fig. 2), we can calculate the impedance [Z] and the admittance [Y] matrices per unit length, necessary to the transmission line analysis. Then we calculate the TWF constants of propagation and scattering parameters, using the procedure described in Appendix I.

By means of the distributed constant equivalent model the TWF study gives results not different from the full-wave analysis [8], [9]. The use of this approximate technique has the advantage of reducing calculation time by a factor of more than 100.

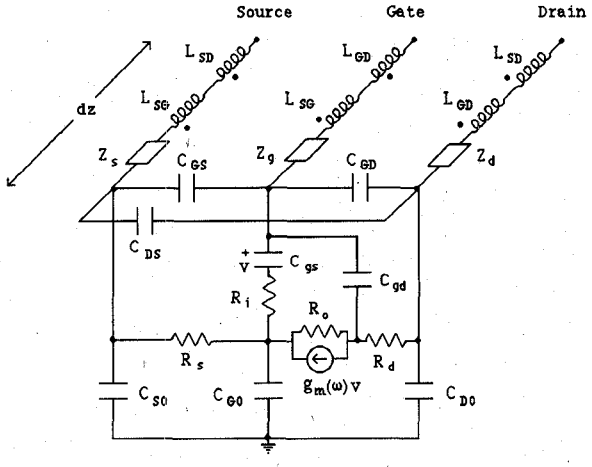

Fig. 2. Equivalent distributed circuit of a TWF section. Z_s, Z_g, and Z_d are the characteristic impedance of the lines. The inductances and the capacitances with capital letters subscript represent the electromagnetic coupling between the electrodes. All the elements represent quantities for unit length.

A. Interelectrode Capacitance and Inductance Matrices

Calculation of the capacitances due to the electrodes is very important for TWF design [1]. So, to calculate the interelectrode capacitance matrix, it is necessary to use an accurate method. Here the moment method [10], [11] has been used, based on a polynomial expansion of the Green's functions calculated with or without the substrate. Even though this method is cumbersome, it has been proved to give results very close to the actual values [12]. The values of the inductance in the circuit of Fig. 2 can be obtained by evaluating the capacitances without the dielectric. In fact, using the hypothesis of quasi-TEM mode propagation, the relation between the capacitance matrix without the dielectric and the inductance matrix is

$$[L] = \frac{[C_0]^{-1}}{v_0^2}$$

where v_0 represents the velocity of light in vacuum. The inductance matrix [L] is also valid with the dielectric present, because of gallium arsenide nonmagnetic behavior.

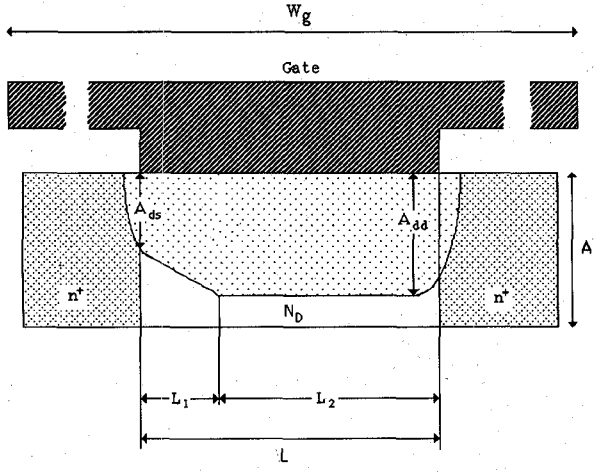

Fig. 3. Cross-section of the gate zone of the TWF.

B. The MESFET Model

The study of TWF active zone is analogous to the common MESFET analysis. The differences regard transconductance determination and that the values of the parameters must be expressed for unit length. In comparison with other studies, this one analyzes carefully the equivalent circuit capacitance, considering the exact geometry of the depletion region under the gate (Fig. 3) [13], [14]. Also capacitances due to the gate shape have been considered. For sake of brevity, only gate-source and gate-drain capacitances formulas are shown for the saturation zone of the FET characteristic. The gate-source (gate-drain) capacitance is the rate of change of free charge on the gate electrode, with respect to the source (drain) bias when the drain (source) and the gate potentials are held fixed:

$$C_{gs} = \frac{qN_D}{2}(A_{dd} - A_{ds})\frac{\partial L_2}{\partial V_s} + \frac{(L - L_2)\epsilon}{2} \cdot \left[\left(1 + \frac{\partial V_{1s}}{\partial V_s}\right)\frac{1}{A_{dd}} + \frac{1}{A_{ds}}\right] + L_2\epsilon\left(1 + \frac{\partial V_{1s}}{\partial V_s}\right)\frac{1}{A_{dd}} + \frac{\pi\epsilon}{2} \quad (1)$$

$$C_{gd} = \frac{qN_D}{2}(A_{dd} - A_{ds})\frac{\partial L_2}{\partial V_d} + \epsilon \sin^{-1} \cdot \left[\left(\frac{V_{bi} - V_{gs} + V_{1s}}{V_{bi} - V_{gs} + V_{ds}}\right)^{1/2}\right] \quad (2)$$

where

$$V_{1s} = \frac{E_s L(V_{gs} - V_t)}{E_s L + V_{gs} - V_t} \quad (3)$$

$$A_{dd} = \left[\frac{2\epsilon(V_{bi} - V_{gs} + V_{1s})}{qN_D}\right]^{1/2}$$

$$A_{ds} = \left[\frac{2\epsilon(V_{bi} - V_{gs})}{qN_D}\right]^{1/2} \tag{4}$$

$$L_2 = \frac{2A}{\pi} \ln\left\{\frac{\pi(V_{ds} - V_{1s})}{2AE_s} + \left[1 + \left(\frac{\pi(V_{ds} - V_{1s})}{2AE_s}\right)^2\right]^{1/2}\right\}. \tag{5}$$

Similar equations can be obtained for the non-saturation zone.

The effect of the third dimension on the device behavior must be analyzed, because the TWF is a few millimeters long whereas common MESFET's are some hundreds of microns long. This fact causes a progressive phase delay as the signal propagates along the gate electrode. Considering the TWF as a succession of many elementary parallel FETs, clearly this phase delay could produce a partial phase cancellation of total current and, as a consequence, a decrease of total transconductance. Including this physical phenomenon, the complete expression of transconductance for unit length is equal to

$$|g_m(\omega)| = g_{mo}\frac{1}{\beta W}\{[1 - \cos(\beta W)]^{1/2} + \sin^2(\beta W)\}^{1/2} \tag{6}$$

$$\arg\{g_m(\omega)\} = \left(\tau + \frac{\beta W}{2}\right) \tag{7}$$

with $\tau = C_{gs}/g_{mo}$ and

$$g_{mo} = \epsilon v_s \left[\frac{qN_D}{2\epsilon(V_{bi} - V_{gs} + V_{1s})}\right]^{1/2}.$$

To obtain amplification it is necessary to reduce gate resistive losses; therefore we used for the gate at T-cross section shape as a simple increase of the gate width (L) produces a remarkable reduction of the transconductance value [1]. Such a shape improves transconductance too: the T-gate reduces the inner inductance of line, and, consequently, the phase delay. Fig. 4 shows the trancon-ductance behavior versus frequency of a "normal" (i.e., parallelepiped) and of a T-gate TWF, calculated from (6). Clearly the T-gate keeps the transconductance value higher with increasing the frequency.

Regarding other elements of the equivalent circuit, such as the internal resistance and the characteristic impedance of the lines, general expressions have been obtained to describe actual device operation accurately. The three electrodes are considered as three coupled microstrips in the presence of a lower ground plane. In order to obtain the drain and source electrode characteristics impedances the following expressions have been used [7]:

$$Z_m = \frac{\Gamma_m}{W_m \delta}\coth(\Gamma_m h) \qquad m = s, d \tag{8}$$

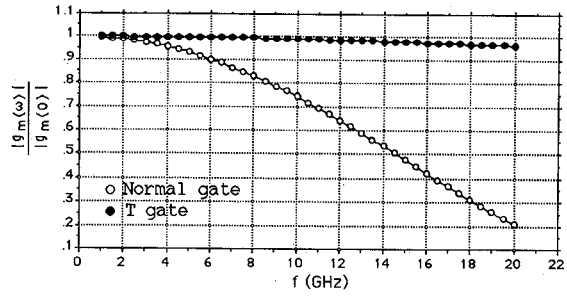

Fig. 4. Transconductance versus frequency of a "normal" (i.e., parallelepiped shape) and "T-gate" TWF.

with

$$\Gamma_m = (1 + j)\sqrt{\delta f \pi \mu_0}.$$

The real and imaginary parts of Z_m represent resistance and inner inductance of the line respectively. The preceding formulas include "skin effect," which reduces the useful cross-section of the conductors when the frequency increases.

Because of gate electrode's position between the source and the drain, its characteristics impedance can be calculated as the parallel combination of two lines, each with half the gate thickness. In this way one obtains

$$Z_g = \frac{\Gamma_g}{2w_{gg}\delta}\coth\left(\frac{\Gamma_g h_g}{2}\right) \tag{9}$$

with

$$\Gamma_g = (1 + j)\sqrt{\delta f \pi \mu_0},$$

$$w_{gg} = \max\{W_g, h\}, \quad h_g = \min\{W_g, h\}.$$

In the T-gate impedance calculation the bar of the T is considered as the strip width.

III. Simulation

Analyzing parasitic capacitances and the MESFET active part, we have obtained general expressions, which are not connected with the characteristics of a particular FET and give, for the first time, an exact mathematical model representing TWF electromagnetic behavior. From this approach, we have developed a computer program, which, starting from the physical dimensions of the electrodes, the active zone doping, and bias, gives the TWF propagation constants.

The structure supports three modes (three forward traveling wave and three reverse) corresponding to three independent eigenvectors (each eigenvalue can be positive or negative). While the first two modes are always lossy, as in a conventional transmission line (i.e., the imaginary part α of k_{iz} is positive), by choosing appropriate physical dimensions, the third mode can have a negative α over some useful bandwidth (Fig. 5). In this way, the mode can grow as the wave travels along the structure.

The analysis of several structures has allowed us to understand the critical physical parameter controlling the

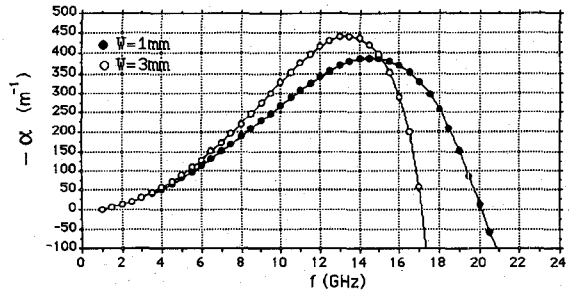

Fig. 5. Coefficient of the imaginary part of the propagation constant k_{iz} $(-\alpha)$ for two different device lengths.

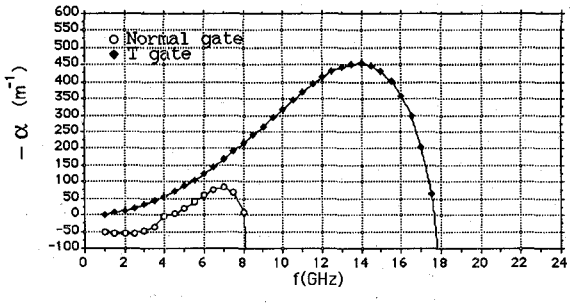

Fig. 6. Comparison of the imaginary part of the propagation constant k_{iz} $(-\alpha)$ between a "normal" (i.e., parallelepiped shape) and "T-gate" TWF.

amplification of the structure. First, the T-gate allows amplification by reducing resistive losses and keeping transconductance value high. Fig. 6 shows $-\alpha$ for both a T-gate and a normal TWF. It is clear that it is very difficult to obtain amplification over a wide bandwidth if a T-gate structure is not used [1].

Moreover, the device amplification increases if an asymmetrical shape of the electrodes is used. In particular, it is necessary to separate the drain from both the gate and the source by 100 μm. To prevent problems of DC dissipation that this distance can cause, a self-aligned configuration with high doped semiconductor on the gate sides has been chosen for the MESFET (Fig. 3). This configuration decreases resistive losses of semiconductor, and it reduces the depletion region spreading in the gate-drain zone, reducing intrinsic capacitances too. A rather high doping of active zone was chosen ($N_D = 3 \cdot 10^{23}$ atoms/m^3). Although it reduces bandwidth by increasing intrinsic capacitances, it produces a higher gain.

Since the results of the simulation program completely depend on the dimensions and physical characteristics of the TWF, it has been possible to optimize such variables. Table I shows the optimized dimensions needed for higher gain over a wide bandwidth.

Fig. 7 shows the eigenvectors (i.e., $\tilde{V}_d$, $\tilde{V}_s$ and $\tilde{V}_g$) of the growing mode for this structure. It is possible to observe that $|\tilde{V}_d|$ is almost null; so, to excite this mode, the TWF must be fed by a signal applied on an extremity of gate electrode and carried out by the other one. The drain can be grounded in both sides, whereas the source is terminated in resistive loads (Fig. 8).

The simulation program also gives the scattering parameters of the TWF, analyzed as a six port structure. The previous consideration about the low value of the modulus of the drain eigenvector allows us (with some calculations) to transform the 6 × 6 [S] matrix in a 4 × 4 matrix. In this way it's possible to use a standard circuit analysis program (Touchstone™) to evaluate the network necessary to feed the device and match to the standard 50 Ω lines.

Fig. 9 shows the global gain obtained with a 3 mm long device, biased in the saturation region (V_{DS} = 4 V, V_{GS} = 0 V). A flat gain of about 8 dB, better than those obtained in previous works [1], [5], [6], is predicted in the range from 7.5 to 14.5 GHz.

TABLE I

Source width	(W_s)	2 μm
Width of gate T-bar	(W_g)	30 μm
Width of gate	(L)	1 μm
Drain width	(W_d)	300 μm
Gate-source distance		10 μm
Gate-drain distance		100 μm
Conductor thickness	(t)	1 μm
Substrate thickness	(h)	30 μm
Active zone thickness	(A)	0.2 μm
TWF length	(W)	3 mm

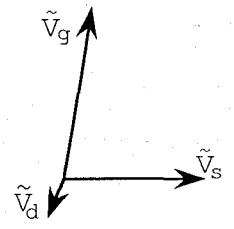

Fig. 7. Eigenvectors configuration of the growing mode for the structure of Table I.

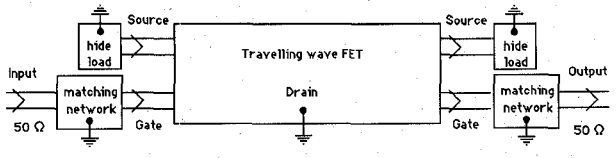

Fig. 8. Practical scheme of the TWF amplifier.

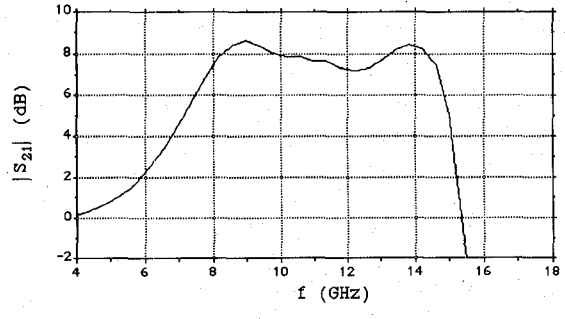

Fig. 9. Gain $|S_{21}|$ versus frequency of the TWF amplifier, obtained by Touchstone™ analysis.

The model also explains the physical phenomenon necessary to obtain amplification. The device can be considered as a succession of elementary FET's, a transverse conduction current flows in each elementary section and depends on the local voltages of the electrodes (i.e., sum

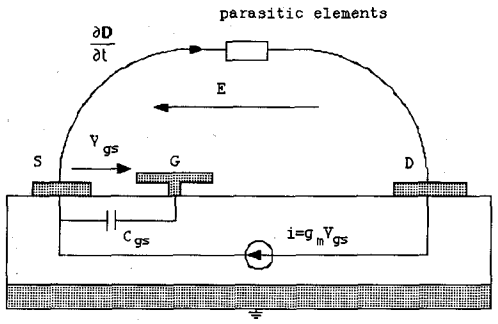

Fig. 10. Essential theoretical scheme of the TWF behavior.

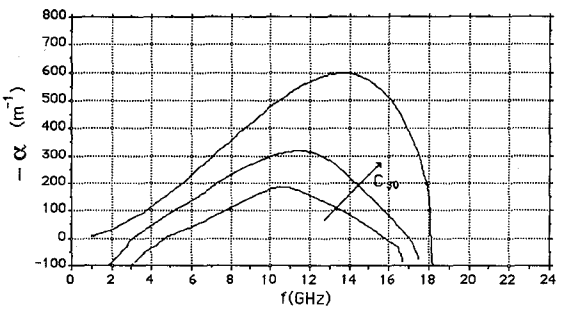

Fig. 11. Imaginary part of the propagation constant k_{iz} $(-\alpha)$ for the growing mode increasing the source-ground capacitance up to 10^{-9} F/m.

of bias and traveling-wave voltage amplitudes). For this reason, a power transfer from the biasing circuit to the traveling wave can occur, if the electric field and variable current are in opposite phase for each TWF section. In this case, referring to Poynting's theorem, the inner product $\boldsymbol{E} \cdot \boldsymbol{J}$ is negative and the energy of the electromagnetic wave increases. From these considerations the necessity of optimizing the electrode geometry, to obtain the maximum power transfer from the bias circuit to the traveling wave, is clearly observed. Looking at the eigenvectors (Fig. 7) we can note that

$$|\tilde{V}_d| < |\tilde{V}_s| < |\tilde{V}_g|,$$

taking into account this relation, an essential scheme can be drawn to justify the previous statements (Fig. 10).

The electric field is directed from drain to source, and the current flows from drain to source controlled by V_{gs} and closes itself as a displacement current across the parasitic elements. The phase relation between this current and the electric field between the source and the gate satisfies the above-mentioned phase condition.

This mechanism explains the excellent theoretical behavior of the amplifier at high frequencies. As the displacement current increases with the frequency the energy exchange improves. This result justifies the addition of some capacitance between drain and source to obtain amplification [5]. We have done some simulations with changing source-ground capacitance (Fig. 11). Such tests showed a considerable improve of the imaginary part of the propagation constant $(-\alpha)$, when source-ground capacitance increases (compare Fig. 11 with Fig. 5).

Such phenomenon can be also explained by considering that an increase of C_{s0} (Fig. 2) balances the high value of the gate junction capacitance C_{gs}. So, it is possible to obtain a matching of wave phase velocities on the two electrodes. Such physical behavior can suggest a change in the TWF configuration: an increase of C_{s0}, by adding a second Schottky contact for the source.

IV. Conclusion

This work shows the possibility of obtaining growing waves in a solid state planar structure and describes a theoretical model and a design method for a TWF. A new amplifier, with a different physical shape, improves previous results [5], [6] and shows it is possible to obtain a wide bandwidth distributed amplifier. Theoretical results pointed out the necessity to use a T-gate structure. For the drain electrode too, it is necessary to reduce resistive losses by increasing electrode width. We can observe the large distance between source and drain, necessary to obtain such propagation conditions and to transfer the power from dc bias circuit to traveling wave. Therefore, TWF requires a very asymmetrical structure. Moreover, to improve TWF performance, changes must be made in the gate, by narrowing the gate width, and its Schottky contact capacitance must also be reduced to increase bandwidth.

To increase performance, further developments of TWF physical configuration can be considered. Particularly, it has been shown that the addition of a new Schottky contact to the source side can yield increases in gain and bandwidth.

Nomenclature

A	Active zone thickness.
A_{dd}	Depletion layer width under the gate near the drain.
A_{ds}	Depletion layer width under the gate near the source.
C_{gd}	Gate-drain capacitance.
C_{gs}	Gate-source capacitance.
E_s	Electric field inducing saturation in the velocity of electronic drift.
$g_m(\omega)$	TWF transconductance.
g_{mo}	FET transconductance.
h	Substrate thickness.
$k_{iz} = \beta - j\alpha$	Constant of propagation of the i mode in the z direction.
L	Width of the lower part of the T gate.
L_1	Width of the non-saturation region.
L_2	Width of the saturation region.
N_D	Doping density of the active zone under the gate.
q	Electronic charge.
t	Conductor thickness.
v_0	Light velocity in vacuum.
V_{1s}	Voltage drop across gate non-saturation zone.
V_{bi}	Built-in voltage.
$V_{gs}(V_{ds})$	Voltage drop between gate-source

(drain-source) under the gate, inside the semiconductor body.

$V_{GS}(V_{DS})$ Voltage between gate-source (drain-source) contacts.

v_s Electronic saturation drift velocity.

$V_s(V_d)$ Source (drain) voltage.

V_t FET Threshold voltage.

W Device length.

W_m Lines' width $m = s, g, d$.

Z_m Characteristic impedance of the TWF lines.

δ Metal conductivity.

ϵ Dielectric permittivity.

τ Switching time of the FET.

Appendix I

Here a quasi-TEM wave propagation is analyzed, starting from the analysis of the equivalent distributed circuits (Fig. 2). Using the Kirchoff laws, the transmission line equations are obtained in matrix form to take account of the three coupled lines:

$$-\frac{\partial \boldsymbol{V}}{\partial z} = [Z]\boldsymbol{I} \tag{A1}$$

$$-\frac{\partial \boldsymbol{I}}{\partial z} = [Y]\boldsymbol{V} \tag{A2}$$

with

$$\boldsymbol{V} = \begin{pmatrix} V_s \\ V_g \\ V_d \end{pmatrix} \quad \boldsymbol{I} = \begin{pmatrix} I_s \\ I_g \\ I_d \end{pmatrix}.$$

The following specific solutions are chosen: $\tilde{\boldsymbol{V}} = \tilde{\boldsymbol{V}}_0 e^{-j(k_z Z + \omega t)}$, where $\tilde{\boldsymbol{V}}$ is the eigenvector, $\tilde{\boldsymbol{V}}_0$ its magnitude and k_z its complex eigenvalue (propagation constant or wave vector). In this way from (A1) and (A2), we have

$$k_z^2[E]\,\tilde{\boldsymbol{V}} = -[Z][Y]\,\tilde{\boldsymbol{V}} \tag{A3}$$

where $[E]$ is the unit matrix. The solution of the eigenvalue problem, expressed by (A3), allows the calculation of the three propagation constants (i.e., k_{iz} $i = 1, 2, 3$) of the three modes propagating in the TWF. The process of analysis consists in getting admittance and impedance matrices of the TWF structure, starting from the equivalent distributed circuit and, then, in solving the eigenvalue problem. This study shows that all eigenvalues are distinct in the TWF. Starting from this observation and using (A1) and (A2), it is possible to obtain the scattering matrix. Equations (A1) and (A2) represent an easily solvable system of equations, by means of Laplace's transform. After some calculations, one obtains the relation (matrix $[T]$) between the input ($z = 0$) currents and voltages, and the output ($z = W$) ones [15]:

$$\begin{pmatrix} \tilde{\boldsymbol{V}}(W) \\ \tilde{\boldsymbol{I}}(W) \end{pmatrix} = [T] \begin{pmatrix} \tilde{\boldsymbol{V}}(0) \\ \tilde{\boldsymbol{I}}(0) \end{pmatrix} \tag{A4}$$

$$[T] = \begin{pmatrix} \sum_{i=1}^{3} \frac{[\hat{Q}_1(p_i)]\cosh(p_i W)}{p_i R(p_i)} & -\sum_{i=1}^{3} \frac{[\hat{Q}_1(p_i)][Z]\sinh(p_i W)}{p_i R(p_i)} \\ -\sum_{i=1}^{3} \frac{[\hat{Q}_2(p_i)][Y]\sinh(p_i W)}{p_i R(p_i)} & \sum_{i=1}^{3} \frac{[\hat{Q}_2(p_i)]\cosh(p_i W)}{p_i R(p_i)} \end{pmatrix} \tag{A5}$$

with

$$R(p_i) = \prod_{\substack{n=1 \\ n \neq i}}^{3} (p_i + p_n)(p_i - p_n)$$

$$[Q_1(p_i)] = p_i^2[E] - [Z][Y]$$

$$[Q_2(p_i)] = p_i^2[E] - [Y][Z]$$

$$p_i = jk_{iz} \qquad i = 1, 2, 3$$

where $[\hat{Q}_1(P_i)]$ and $[\hat{Q}_2(P_i)]$ are the adjoint of $[Q_1(P_i)]$ and $[Q_2(P_i)]$. Knowing the matrix $[T]$, it is possible to obtain the TWF open-circuit impedance matrix $[Z_{oc}]$. To make calculations easier, matrix [T] can be partitioned as

$$[T] = \begin{pmatrix} [A] & [B] \\ [C] & [D] \end{pmatrix}.$$

After some algebraic manipulation one obtains

$$[Z_{oc}] = \begin{pmatrix} -[C]^{-1}[D] & -[C]^{-1} \\ [B] - [A][C]^{-1}[D] & -[A][C]^{-1} \end{pmatrix}. \tag{A6}$$

From (A6) we easily have the scattering matrix $[S]$, because of

$$[S] = ([Z_{oc}] - [\eta])([Z_{oc}] + [\eta])^{-1} \tag{A7}$$

where the diagonal matrix $[\eta]$ represents the impedance matrix of TWF port lines.

By using the described procedure we can determine the scattering matrix of TWF, considered as a six port structure. The TWF scattering matrix has the following symmetry:

$$[S] = \begin{pmatrix} [S_1] & [S_2] \\ [S_2] & [S_1] \end{pmatrix}$$

where matrices $[S_1]$ and $[S_2]$ have 3×3 dimensions and matrix $[S]$ has 6×6 dimensions. Such symmetry can be easily explained by examining the TWF itself, because

one obtains the same electromagnetic configuration by exchanging input and output lines.

References

[1] G. D'Inzeo, R. Giusto, and C. Petrachi, "Active devices for microwave distributed amplification," *Microwave and Optical Technology Letters*, vol. 3, pp. 51–54, Feb. 1990.

[2] G. McIver, "A traveling wave transistor," *Proc. IEEE*, vol. 53, pp. 1747–1748, Nov. 1965.

[3] A. Podgorski and L. Y. Wey, "Theory of traveling wave transistor," *IEEE Trans. Electron Devices*, vol. ED-29, pp. 1845–1853, Dec. 1982.

[4] C. J. Wei, "Novel design of traveling wave FET," *Electron. Lett.*, vol. 19, pp. 461–463, June 1983.

[5] A. J. Holden, D. R. Daniel, I. Davies, C. H. Oxley and H. D. Rees, "Gallium arsenide traveling-wave field-effect transistor," *IEEE Trans. Electron Devices*, vol. ED-32, pp. 61–66, Jan. 1985.

[6] N. Sebati, P. Gamand, C. Varin, F. Pasqualini, and J. C. Meunier, "Continuous active T-gate traveling-wave transistor," *Electron. Lett.*, vol. 25, pp. 403–404, Mar. 1989.

[7] W. Heinrich, "Distributed equivalent-circuit model for traveling-wave FET design," *IEEE Trans. Microwave Theory Tech.*, vol. MTT-35, pp. 487–491, May 1987.

[8] W. Heinrich and H. L. Hartnagel, "Wave propagation on MESFET electrodes and its influence on transistor gain," *IEEE Trans. Microwave Theory Tech.*, vol. MTT-35, pp. 1–8, Jan. 1985.

[9] W. Heinrich and H. L. Hartnagel, "Field theoretical analysis of wave propagation on FET electrodes including losses and small-signal amplification," *Int. J. Electron.*, vol. 58, pp. 613–627, Apr. 1985.

[10] R. F. Harrington, "Matrix methods for field problems," *Proc. IEEE*, vol. 55, pp. 136–149, Feb. 1967.

[11] ——, *Field Computation by Moment Methods*. New York: Macmillan, 1968.

[12] A. Farrar and A. T. Adams, "Characteristic impedance of microstrip by the method of moments," *IEEE Trans. Microwave Theory Tech.*, vol. MTT-18, pp. 65–66, Jan. 1970.

[13] M. S. Shur, "Analytical Model of GaAS MESFET's," *IEEE Trans. Electron Devices*, vol. ED-25, pp. 612–618, June 1978.

[14] T. H. Chen and M. S. Shur, "A Capacitance Model for GaAs MESFET's," *IEEE Trans. Electron Devices*, vol. ED-12, pp. 883–891, May 1985.

[15] S. Frankel, Ed., *Multiconductor Transmission Line Analysis*. Menlo Park, NJ: S. Frankel and Assoc., 1976.

Stefano D'Agostino was born in Rome, Italy, in 1961. He received the degree in electronic engineering from the University of Rome, "La Sapienza" in 1986.

In 1987 he was an engineering employee at the Elettronica S.p.A. as a Staff Member specializing in the area of ECM systems. Since 1989 he has worked at the University of Rome, "La Sapienza," Department of Electronics. His research has encompassed both theoretical and experimental studies of most semiconductor devices, including wideband amplifiers such as distributed and traveling wave. His most recent work is in the field of monolithic microwave integrated circuits.

Dr. D'Agostino is a member of AEI.

Guglielmo D'Inzeo (M'83) was born in Milan, Italy, in 1952. He received the Laurea degree in electronic engineering from the University of Rome in 1975.

In 1976 he joined the Department of Electronics at the University of Rome. He was Professore Incaricato at the University of Calabria (1979–1981) and at the University of Ancona (1980–1985). In 1986 he became Associate Professor of Microwaves Measurement at the "La Sapienza," University of Rome. Currently he is Full Professor of Bioelectromagnetics Interaction at the same University. His research activity deals active and passive microwave components, interaction of electromagnetic fields with tissues, and biological effects of microwaves and ELF fields.

Dr. D'Inzeo is a member of the board of EBEA (European Bioelectromagnetics Association).

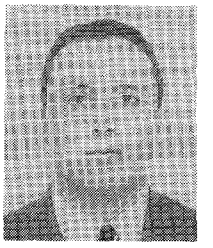

Luca Tudini was born in Rome, Italy, on August 18, 1964. He received the degree in electronic engineering from the University of Rome, "La Sapienza."

Since then, he has been working at the University of Rome, in the field of active microwave components characterization.